3D FEM-BEM coupled resolution for acoustic waves propagation in potential flow

Nolwenn Balin, Guillaume Sylvand, Fabien Casenave

3D FEM-BEM coupled resolution for acoustic waves propagation in potential flow

N. Balin[a], G. Sylvand[a] and F. Casenave[b]

[a]EADS France, Batiment Campus Engineering / Service IW/SE/MA, BP 90112, 31703 Blagnac Cedex, France

[b]Centre d'Enseignement et de Recherche en Mathématiques et Calcul Scientifique, 6 et 8 avenue Blaise Pascal Cité Descartes - Champs sur Marne 77455 Marne la Vallée Cedex 2

nolwenn.balin@eads.net

In order to reduce the environmental impact of aircraft, it is necessary to accurately simulate acoustics waves propagation in a complex environment. A classical method used to compute the noise propagation on large distances is the Boundary Element Method (BEM). However this method is restricted to a uniform flow. To improve the level of modeling, we present here a coupling between Finite Element (FEM) and Boundary Element Methods to solve the acoustic propagation problem that consists in a potential flow near the aircraft and a uniform flow far-away from the aircraft. The Lorentz transformation is introduced in the exterior domain to easily use the Boundary Element Method for the uniform flow. This transformation is also applied in the interior domain to obtain a natural coupling between the two domains. 3-D numerical results representative of various configurations, and in particular results with modal acoustic sources in the potential flow, are shown.

1 Introduction

Under environmental pressures, aircraft manufacturers have developed tools to simulate acoustic waves propagation. Computing acoustics in flows with zero or uniform velocity can be inaccurate and non-physical, as the flow around civil aircraft often reaches Mach 0.8 and installation effects occur, due to the wings for instance. Then, introducing a volume around the turbofan, where more complex flows can be treated, and coupling it with an exterior Helmholtz problem appears as a pertinent way to improve existing simulation tools. This method allows to take into account the modifications of the convective carrier flow due to the presence of rigid objects and the use of a powerful method for long range propagation will allow us to take into account installation effects.

This work is the 3D extension to Duprey's PhD thesis [1].

2 Physical model problem

2.1 Model problem

Three flow areas can be identified in our case (cf. Fig. 1):

1. complex viscous flow with compression, combustion and expansion and the boundary layers (1' area on Fig. 1),
2. potential flow,
3. uniform flow.

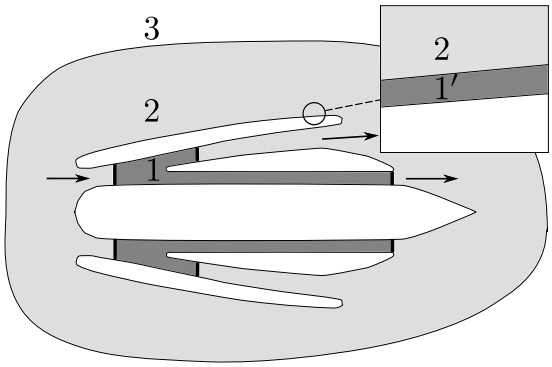

Figure 1: Air flux in a civil turbofan

The sound is produced as a result of all the complex phenomena occurring in zone 1. In our study, we will consider them as inputs. Motorists can produce models for the engine sound generation, that often consist in acoustic modes at the limit of zone 1. Then, difficulties specific to this zone will not be treated here, and we will focus on the acoustic propagation in the potential and uniform flows.

The potential flow assumption can be discussed for the outgoing air flux. However, this assumption can be valid for the front part of the turbofan and for some configuration it can give reasonable results or at least starting points for an improved method that uses the potential approximation results.

The objective is to obtain the acoustic pressure around the object. For that, following the potential assumption, we define a scalar field ψ such that $\overrightarrow{V} = \overrightarrow{\nabla\psi}$ with $\overrightarrow{V}$ the flow velocity.

The model problem that we consider is represented on Fig. 2.

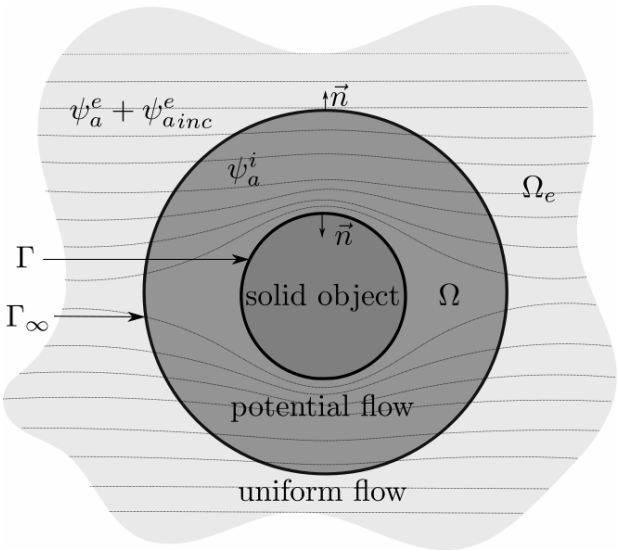

Figure 2: Notations and conventions

2.2 Acoustic equations

The flow quantities are split in acoustic and flow quantities (with respectively indices "a" and "0").

The acoustic potential ψ_a is defined as the solution of the linearized Euler equations in the frequency domain [2]:

- in domain Ω_e (uniform flow):

$$k_\infty^2 + \Delta\psi_a + 2ik_\infty \overrightarrow{M_\infty} \cdot \overrightarrow{\nabla\psi_a} - \overrightarrow{M_\infty} \cdot \overrightarrow{\nabla}(\overrightarrow{M_\infty} \cdot \overrightarrow{\nabla\psi_a}) = 0. \quad (1)$$

- in domain Ω (potential flow):

$$\rho_0 \left(k_0^2\psi_a + ik_0\overrightarrow{M_0} \cdot \overrightarrow{\nabla\psi_a}\right) + \mathrm{div}\left(\rho_0 \left(\overrightarrow{\nabla}\psi_a + ik_0\psi_a\overrightarrow{M_0}\right)\right) - \mathrm{div}\left(\rho_0 \left(-(\overrightarrow{\nabla}\psi_a \cdot \overrightarrow{M_0})\overrightarrow{M_0}\right)\right) = 0 \quad (2)$$

where $\overrightarrow{M_0}$ stands for the Mach vector, k the wavenumber, ρ_0 the volume density and ψ_a the acoustic potential. Notice that all quantities occuring in Eq. 2 are not uniform in space Only subsonic flows are considered.

Using linearized Bernoulli equation it is possible to recover the acoustic pressure and velocity from the acoustic potential:

$$p_a = -\rho_0 c_0 \left(-ik\psi_a + \overrightarrow{M_0} \cdot \overrightarrow{\nabla\psi_a}\right) \tag{3}$$

$$\overrightarrow{V_a} = \overrightarrow{\nabla\psi_a} \tag{4}$$

3 Problem formulation

3.1 Variational formulation in the potential flow domain

We formulate Eq. (2) in a weak form:

$$\begin{aligned}\int_{\Omega_i} \rho_0 \left[\overrightarrow{\nabla\psi_a} \cdot \overrightarrow{\nabla\psi^t} - k_0^2 \psi_a \psi^t - (\overrightarrow{M_0} \cdot \overrightarrow{\nabla\psi_a})(\overrightarrow{M_0} \cdot \overrightarrow{\nabla\psi^t})\right] d\omega \\ - \int_{\Omega_i} ik_0\rho_0 \left((\overrightarrow{M_0} \cdot \overrightarrow{\nabla\psi_a})\psi^t - (\overrightarrow{M_0} \cdot \overrightarrow{\nabla\psi^t})\psi_a\right) d\omega \\ - \int_{\Gamma_\infty} \rho_0 \left(\overrightarrow{\nabla}\psi_a \cdot \overrightarrow{n} - (-ik_0\psi_a + \overrightarrow{\nabla}\psi_a \cdot \overrightarrow{M_0})(\overrightarrow{M_0} \cdot \overrightarrow{n})\right)\psi^t d\gamma = 0\end{aligned} \tag{5}$$

Γ_∞ is the boundary between Ω and Ω_e domains and we will use a Boundary Element Method to obtain an expression for the integral on Γ_∞.

3.2 Formulation in the uniform flow domain

As in Ω_e the flow is supposed uniform, we introduce the Lorentz transformation to reduce Eq. (1) to the Helmholtz equation. This transformation is composed of :

- a space transformation s

$$s\left(\overrightarrow{OP}\right) = \overrightarrow{OP} + C\left(\overrightarrow{OP} \cdot \overrightarrow{M}_\infty\right)\overrightarrow{M}_\infty \tag{6}$$

with $C = \frac{1}{M_\infty^2}\left(\frac{1}{\sqrt{1-M_\infty^2}} - 1\right)$.

- a change of phase $\mathcal{P}$:

$$\mathcal{P}\phi\left(\overrightarrow{y}\right) = \phi\left(\overrightarrow{y}\right) e^{\frac{ik_\infty \overrightarrow{M}_\infty \cdot \overrightarrow{y}}{\sqrt{1-M_\infty^2}}} \tag{7}$$

Applying this transformation, the problem is written in terms of $\overrightarrow{x}' = s\left(\overrightarrow{x}\right)$. Consider now the unknowns defined by $q = \mathcal{P}\psi_a \circ s^{-1}$ and $\lambda = \dfrac{\partial q}{\partial n}$ on Γ_∞.

As the equation to solve in Ω_e is now the Helmholtz equation, we can use the integral representation theorem and the problem reduces to a variational formulation on the boundary Γ_∞:

$$\int_{\Gamma_\infty} \left[D^*(\lambda) - N(q) + \frac{1}{2}\lambda\right] q^t = \int_{\Gamma_\infty} \frac{\partial q^e_{a_{\text{inc}}}}{\partial n} q^t \tag{8}$$

$$\int_{\Gamma_\infty} \left[S(\lambda) - D(q) + \frac{1}{2}q\right] \lambda^t = \int_{\Gamma_\infty} q^e_{a_{\text{inc}}} \lambda^t \tag{9}$$

where $q^e_{a_{\text{inc}}}$ is the transformed acoustic potential created by the source and operators D, D^*, S and N are the integral operators arising in Helmholtz integral equations [3].

3.3 Coupled problem

As we impose that on Γ_∞ the flow quantities are identical for Ω and Ω_e, the coupling conditions between the domains Ω and Ω_e are, $\forall x \in \Gamma_\infty$,

$$q_{|\Omega}(x) = q_{|\Omega_e}(x) \qquad \frac{\partial q_{|\Omega}}{\partial n}(x) = \frac{\partial q_{|\Omega_e}}{\partial n}(x) \tag{10}$$

Using the Lorentz transformation also in the potential domain Ω, the surfacic integral on Γ_∞ of Eq. 5 can be identified with one of the integral arising in the previous Eq. (8).

The two domains can then be solved using a Levillain's S-formulation [4, 5]:

$$\begin{cases} a(q, q^t) + \displaystyle\int_{\Gamma_\infty} D^*\left(\frac{\partial q}{\partial n}\right) q^t - \int_{\Gamma_\infty} N(q)\, q^t \\ \qquad\qquad - \dfrac{1}{2}\displaystyle\int_{\Gamma_\infty} \frac{\partial q}{\partial n} q^t = \int_{\Gamma_\infty} \frac{\partial q^e_{inc}}{\partial n} q^t \\ \\ -\displaystyle\int_{\Gamma_\infty} S\left(\frac{\partial q}{\partial n}\right)\lambda^t + \int_{\Gamma_\infty} D(q)\,\lambda^t - \frac{1}{2}\int_{\Gamma_\infty} q\lambda^t = -\int_{\Gamma_\infty} q^e_{inc}\lambda^t \end{cases} \tag{11}$$

with $a(\cdot,\cdot)$ the bilinear operator of the volumic part defined by

$$\begin{aligned} a(q, q^t) = \int_\Omega \frac{\rho_0}{\rho_\infty} \Big[\overrightarrow{\mathcal{L}_- q} \cdot \overrightarrow{\mathcal{L}_+ q^t} - {k_0}^2 q q^t \\ - ik_0 \left(\overrightarrow{M_0} \cdot \overrightarrow{\mathcal{L}_- q}\right) q^t - ik_0 \left(\overrightarrow{M_0} \cdot \overrightarrow{\mathcal{L}_+ q^t}\right) q \\ - \left(\overrightarrow{M_0} \cdot \overrightarrow{\mathcal{L}_- q}\right)\left(\overrightarrow{M_0} \cdot \overrightarrow{\mathcal{L}_+ q^t}\right)\Big] \end{aligned} \tag{12}$$

and

$$\left(\overrightarrow{\mathcal{L}_\pm f}\right) = \overrightarrow{\nabla} f + \left[C\left(\overrightarrow{M}_\infty \cdot \overrightarrow{\nabla} f\right) \pm \frac{ik_\infty}{1 - M_\infty^2} f\right]\overrightarrow{M}_\infty. \tag{13}$$

This coupled variational formulation is well-posed as shown in [6].

3.4 Modal excitation

We will now consider the modeling of a modal source included in the potential domain (the flow is however supposed uniform on the modal surface Γ_M). The unknowns q and λ on Γ_M can be expressed as a sum of incident and reflected modes:

$$p = \sum_{m=0}^{M}\sum_{n=1}^{minc} \alpha_{mn} u^{inc}_{mn} + \sum_{m'=0}^{M}\sum_{n'=1}^{mdiff} \beta_{m'n'} u^{diff}_{m'n'} \tag{14}$$

$$\frac{\partial p}{\partial n} = \sum_{m=0}^{M}\sum_{n=1}^{minc} \alpha_{mn} \frac{\partial u^{inc}_{mn}}{\partial n} + \sum_{m'=0}^{M}\sum_{n'=1}^{mdiff} \beta_{m'n'} \frac{\partial u^{diff}_{m'n'}}{\partial n} \tag{15}$$

with u^{inc}_{mn} and $u^{diff}_{m'n'}$ the modal basis that depends on the shape of the modal duct and α_{mn} and $\beta_{m'n'}$ the amplitude coefficients for the modes. α_{mn} are known whereas $\beta_{m'n'}$ are unknown. It is then possible to formulate the problem in order to determine $\beta_{m'n'}$.

The Dirichlet-Neumann condition on Γ_M can be expressed by

$$-\frac{1}{ik}\frac{\partial u^{\text{inc}}_{m,n}}{\partial n} = Y_{m,n} u^{\text{inc}}_{m,n}, \qquad -\frac{1}{ik}\frac{\partial u^{\text{diff}}_{m'n'}}{\partial n} = Y_{m'n'} u^{\text{diff}}_{m'n'} \tag{16}$$

with Y_{mn} and $Y_{m'n'}$ impedance coefficients that depend on the mode.

We then obtain (if we consider only the coupling with the FEM model and the modal surface) the following variational formulation

$$a(q,q^t) - \sum_{m,n} \beta_{m,n} Y_{m,n} \int_{\Gamma_M} u^{\text{diff}}_{m,n} q^t = -\sum_{m',n'} \alpha_{m'n'} Y_{m'n'} \int_{\Gamma_M} u^{\text{inc}}_{m',n'} q^t \quad (17)$$

4 Numerical simulation

This study has lead to the production of a code, incorporated in EADS-IW acoustic wave propagation software. P_0 finite elements are used for unknowns λ and P_1 finite elements for unknowns q. A fast multipole solver (FMM) [7] can be used to solve the dense linear part of the system due to the use of BEM.

Many test cases, from validation to pseudo-industrial configurations, have been conducted, sometimes on a large number of processors.

4.1 Cylindrical duct with uniform flow

Consider a modal cylindrical duct of length $L = 1$ m and radius $R = 0.25$ m. The flow is uniform, in the direction of the duct, with a Mach number of 0.8. The frequency of the source is 1020Hz. (Fig. 3).

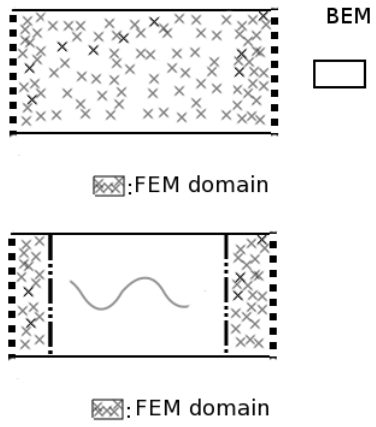

Figure 3: Some FEM-BEM configurations for the validation on a cylindrical duct

Four kinds of computation have been performed:

- classical BEM pressure formulation of ACTIPOLE,
- potential BEM formulation,
- potential FEM formulation.
- potential coupled FEM-BEM formulation,

Comparisons have been carried out on the reflection coefficients of the mode and the pressure predicted in the duct. For instance, the comparison of the pressure field in the duct predicted by the potential and the pressure BEM formulations on this test case has shown a 2% error in L^2-norm. Due to finite element dispersion, the mesh must be refined in the FEM part. Convergence studies are running.

The full FEM formulation allows to compare the configuration of different flows between the modal surface and the external domain Ω_e with reference solution.

4.2 Fan model problem

We now consider a fan model problematic represented Fig. 4. It consists in an annular duct with an infinite hub, two flows considered as uniform without transition layer. We will present here only results for the case where the two flows are identical.

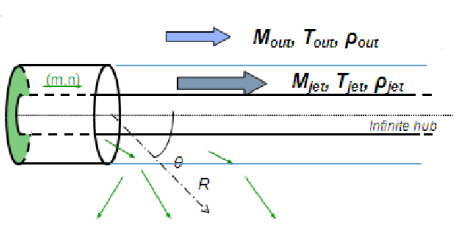

Figure 4: Fan problematic model problem

The inner radius is 0.6 m and the outer radius is 1.2 m. The frequency of interest is 500 Hz and the flow velocity is defined with a Mach number of 0.6. We will compare an analytic solution (without Kutta condition) with the solution given by the method proposed here. To simulate this problem with a FEM-BEM approach, the infinite hub has been truncated at a distance of 7.2 m and the FEM domain consists in the jet flow but restricted to a distance of 6.8 m from the trailing edge near the modal surface. The receivers are located on a arc circle ($\theta = 0°$ corresponds to the hub direction, $\theta = 180°$ to the backward direction).

Figs. 5 and 6 show the comparison of the two methods for two modes and the RMS sum on all the propagative modes.

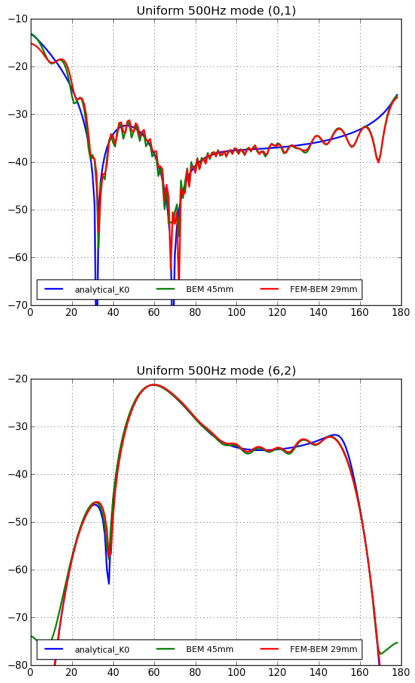

Figure 5: FEM-BEM results for modes (0,1) and (6,2)

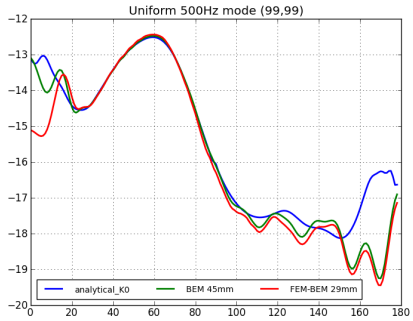

Figure 6: FEM-BEM RMS results

Globally we have a good agreement between the two methods. The main differences between the two methods are in the hub direction and in the backward direction. These differences are due to the truncation of the hub. A mesh with 2.5 millions of volumic and 320 000 surfacic unknowns has been used for this simulation. The FMM solver has been selected and a residual of 10^{-5} has been reached in 81 iterations.

4.3 Potential flow around a sphere

Consider a test case with a rigid sphere in a Mach 0.4 flow going up, and an acoustic source consisting of a "potential" monopole above the sphere. We consider two configurations:

1. non physical case where the flow is uniform,
2. the flow is uniform outside the white "circle" and potential inside, continuity across this "circle" is verified.

In this example, the presence of a more realistic flow around the sphere has modified the potential map as shown Fig. 7. Local acoustic velocity and pressure magnitude have increased, as well as its magnitude in the shadow zone.

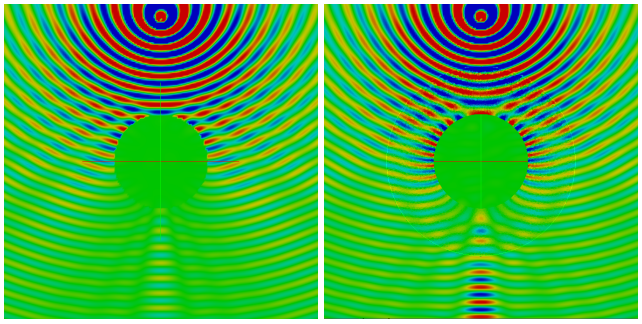

Figure 7: Acoustic total pressure
(*left* uniform flow BEM, *right* potential flow FEM-BEM)

5 Conclusion

A coupled BEM-FEM formulation for the problem of acoustic propagation in a mixed potential and uniform flow has been written. This formulation has been implemented into an industrial software that allows to take into account realistic 3D configurations. It has also been validated on canonical test cases, for which analytic references were available, and more realistic test cases, for which the influence of the potential flow is visible.

Some tests must still be performed. First to determine the capabilities of this method to take into account a configuration with a non-potential flow. These capabilities must be measured from the observable point of view for configurations representative of industrial test cases. Secondly, further tests are needed to explore the meshing requirements.

Acknowledgments

This work takes part in the AEROSON project, financed by the ANR (French National Research Agency).

References

[1] S. Duprey. *Analyse Mathématique et Numérique du Rayonnement Acoustique des Turboréacteurs*. PhD thesis, Nancy, 2005.

[2] E Peynaud. Modélisation numérique du rayonnement acoustique de turboréacteurs. Master's thesis, INSA Toulouse, 2009.

[3] I. Terrasse, T. Abboud, *Modélisation des phénomènes de propagation d'ondes* Ecole Polytechnique, 2007.

[4] V. Levillain, *Couplage eléments finis-équations intégrales pour la résolution des équations de Maxwell en milieu hétérogène*. PhD thesis, 1991.

[5] F Casenave. Couplage BEM-FEM 3D pour la simulation du bruit rayonné par un turboréacteur. Master's thesis, ENPC, 2010.

[6] F Casenave. *3D Coupled resolution of acoustics waves propagation between a potential flow and a uniform flow*. Waves Conference, 2011.

[7] Guillaume Sylvand. *La méthode multipôle rapide en électromagnétisme. Performances, parallélisation, applications.* PhD thesis, École National des Ponts et Chaussées, June 2002.